Central European Journal of Energetic Materials
ISSN 1733-7178; e-ISSN 2353-1843

Cent. Eur. J. Energ. Mater. 2021, *18*(3): 369-384; DOI 10.22211/cejem/142572
Article is available in PDF-format, in colour, at:
https://ipo.lukasiewicz.gov.pl/wydawnictwa/cejem-woluminy/vol-18-nr-3/

Research paper

Green Fabrication of Nanoscale Energetic Molecular Perovskite $(H_2dabco)[Na(ClO_4)_3]$ with Reduced Mechanical Sensitivity

Li-shuang Hu[1,*)], Zelin Du[1)], Yang Liu[1,)], Shida Gong[1)], Chunyu Guang[1)], Xin Li[1)], Zhi Yang[1)], Qi Jia[2)], Kaili Liang[1)]**

[1)] *School of Environment and Safety Engineering, North University of China, Taiyuan 030051, China*
[2)] *Norinco Group Test and Measuring Academy, Huayin 714200, China*
**E-mails:* hlsly1314@163.com; ** lyang1150@126.com

Abstract: High-energy-density molecular perovskite energetic materials with high detonation performance have attracted much attention, but poor safety performance has limited their potential applications. In this paper, nano sodium perchlorate-based molecular perovskite $(H_2dabco)[Na(ClO_4)_3]$ (nano DAP-1) was fabricated by green ball-milling technology. The structure and morphology of the samples were characterized and the results showed that nano DAP-1 with nearly spherical morphology has a narrow particle size distribution, < 1 μm. The thermal decomposition properties were investigated by differential scanning calorimetry (DSC). The exothermic peak of nano DAP-1 thermal decomposition was 330.0 °C, a decrease of 51.7 °C compared with that of raw DAP (381.7 °C). The apparent activation energy (E_a) of nano DAP-1 was calculated to be 160.9 kJ·mol^{-1}, which is lower than that of raw DAP-1 (168.6 kJ·mol^{-1}). Mechanical sensitivity studies showed that nano DAP-1 (H_{50}: 64 cm) exhibited a lower impact sensitivity than that of the raw DAP-1 (H_{50}: 51 cm). This work provides a simple and effective way for improving the thermal decomposition properties and safety performance of molecular perovskite energetic materials.

Keywords: molecular perovskite, $(H_2dabco)[Na(ClO_4)_3]$, ball-milling, thermal decomposition, mechanical sensitivity

1 Introduction

The development of new explosives with high detonation performance and good safety performance has attracted much attention from domestic and international experts. Being different from the traditional high-energy small organic molecule explosives, novel classes of energetic materials have been prepared to meet future requirements, such as nitrogen-rich molecules [1-4], energetic salts [5-8], energetic co-crystals [9-11], energetic coordination polymers [12, 13], metal-organic frameworks and so on. It is of great significance to develop a new generation of weapons and ammunitions based on the high-energy insensitive properties of energetic materials.

Recently, molecular perovskite energetic materials, combining an inorganic oxidizer and an organic fuel into a ternary highly symmetric unit, was introduced by Chen's group [14-16]. A series of perchlorate-based molecular perovskite energetic materials $(H_2dabco)[M(ClO_4)_3]$ (M = Na^+, K^+, Rb^+, and NH_4^+) was designed and prepared by molecular assembly strategy. The excellent detonation performance, good thermostability and even low cost show great advantages for practical applications. In particular, the detonation velocity and detonation pressure of molecular perovskite energetic materials, which are key factors in evaluating the mechanical properties of energetic materials, are higher than those of the traditional nitramine explosives, such as 1,3,5-trinitro-1,3,5-triazinane (RDX) and 1,3,5,7-tetranitro-1,3,5,7-tetrazocane (HMX), and are almost the same as those of 2,4,6,8,10,12-hexanitro-2,4,6,8,10,12-hexaazatetracyclo[5.5.0.$0^{3,11}$.$0^{5,9}$]dodecane (CL-20) [14]. Additionally, the low-cost feature gives unlimited possibilities in advanced and smart weapons [17-23]. However, their poor safety performance seriously limits their application at a deeper level [24-28]. Therefore, it is interesting and valuable to develop a green and efficient method to enhance the safety performance of molecular perovskite energetic materials.

Ball-milling technology, as a green and efficient top-to-down method, has been used widely to refine ultrafine energetic material particles and to achieve reduced sensitivity of energetic materials [29-32]. During the milling process, the particles with irregular morphologies and sizes are crushed, ground and ripened, and then ultimately transformed into sphericized particles. Nano-sized spherical particles can reduce the initiation probability easier than that of irregular particles, when they are subjected to external mechanical stimuli [33]. Thus, this is a potential and prospective way to reduce the sensitivity of molecular perovskite energetic materials.

Molecular perovskite $(H_2dabco)[Na(ClO_4)_3]$ (DAP-1), as a typical and important member of the perchlorate-based molecular perovskite energetic materials group, has a high detonation velocity (9306 $m \cdot s^{-1}$), high detonation pressure (48.3 GPa) and high detonation heat (8.89 $kJ \cdot g^{-1}$), which offers great potential for future applications [14, 15]. However, its weak safety performance (impact sensitivity: 17 J; friction sensitivity: 36 N) cause a huge obstacle.

In the present work, mechanical ball-milling technology was introduced to prepare nano DAP-1, aimed at reducing the mechanical sensitivity. The morphology and structure of DAP-1 before and after ball-milling treatment were studied. The thermal decomposition performance of as-obtained samples is discussed and the mechanical sensitivity was evaluated. This work can offer a new way to promote the further application of molecular perovskite energetic materials in advanced explosive and propellant fields.

2 Experimental

2.1 Materials and preparation

The sodium perchlorate ($NaClO_4$) and perchloric acid ($HClO_4$, 70%) were provided from Shanxi Jiangyang Chem. Eng. Co., Ltd. 1,4-Diazabicyclo[2.2.2]octane (dabco, $C_6H_{12}N_2$) was provided by Shanghai Aladdin Biochemical Technology Technology Co., Ltd.

Molecular perovskite $(H_2dabco)[Na(ClO_4)_3]$ (DAP-1) was fabricated by the molecular assembly strategy. Briefly, $NaClO_4$ (1 mmol), dabco (1 mmol), and H_2O (0.163 mL) containing $HClO_4$ (2 mmol) were added to deionized water (20 mL). The components dissolved completely and naturally crystallised at room temperature. The samples were obtained after filtration, washing, and drying.

Nano DAP-1 samples were prepared by the mechanical ball-milling method. Raw DAP-1 (5 g) and zirconia beads (15 g) of different sizes were added together to the ball-milling apparatus. A rotational speed of 500 rpm was maintained for 6 h. Nano DAP-1 samples were obtained after filtration and drying.

2.2 Characterization

Powder X-ray diffraction (XRD) patterns were recorded on a Philips X'Pert Pro X-ray diffractometer (PANalytical, Holland). Scanning electron microscopic (SEM) images were collected using an Ultra 55 microscope (Zeiss, Germany). Fourier transform infrared (FT-IR) spectra of the samples were

recorded with a Thermo Scientific Nicolet iS10 spectrophotometer (Thermo Scientific, USA) in the range 650-4000 cm^{-1}.

Thermal performance analysis was performed on a STA449F3 Jupiter thermos-gravimetric differential scanning calorimeter (TG-DSC, Netzsch, Germany) with a temperature range of 40~500 °C, at heating rates of 5, 10, 15, and 20 °C·min^{-1}.

The impact sensitivity was evaluated based by GJB-772A-1997. The impact sensitivity was tested with a WL-1 type impact sensitivity apparatus. The special height (H_{50}) value represents the height from which a 2.5 ±0.002 kg drop-hammer will result in an explosive event in 50% of the trials. 25 drop tests were conducted to calculate H_{50} with 35 ±1 mg samples.

Caution! DAP-1 samples are hazardous because of high friction *sensitivity.* Therefore, the sample size was reduced as far as possible for safety during this experiment. The friction sensitivity experiments were measured with a MGY-1 type friction sensitivity instrument. A probability of explosion (P) was given from 25 tests. Suitable masses of 10 mg were tested with a 2 kg pendulum hammer, below a 90° tilt angle and 3.0 MPa pressure.

3 Results and Discussions

The structure and morphology of the samples were characterized, and Figure 1 shows the SEM images and XRD patterns of raw DAP-1 and nano DAP-1. The structure of raw DAP-1 shows a three-dimensional block structure around 100 μm, and macroparticles with cluster growth were observed. However, after green ball-milling, nano DAP-1 was obtained with nearly spherical morphology having a narrow particle size distribution, <1 μm, as shown in Figure 1(c). The organic-inorganic hybrid perovskite structure of DAP-1 is shown in Figure 1(d). Figure 1(e) shows the XRD patterns of raw and nano DAP-1, as well as the simulated pattern. The peak positions of the samples and the simulation data are almost identical, despite their differing diffraction intensities. The main diffraction peaks were located at 12.70°, 21.75°, 25.16°, and 38.10°, which correspond to the crystal planes (222), (400), and (600), respectively. This showed that the crystal structure of the sample before and after ball-milling had not changed. Compared with the raw material, the nanomaterial had intensity changes in the main characteristic peaks. This is because the nanoscale sample obtained shows different exposed surfaces of the particles, which is different from those of raw DAP-1. The above results indicated that the nanoscale energetic molecular perovskite can be obtained via the ball-milling technique.

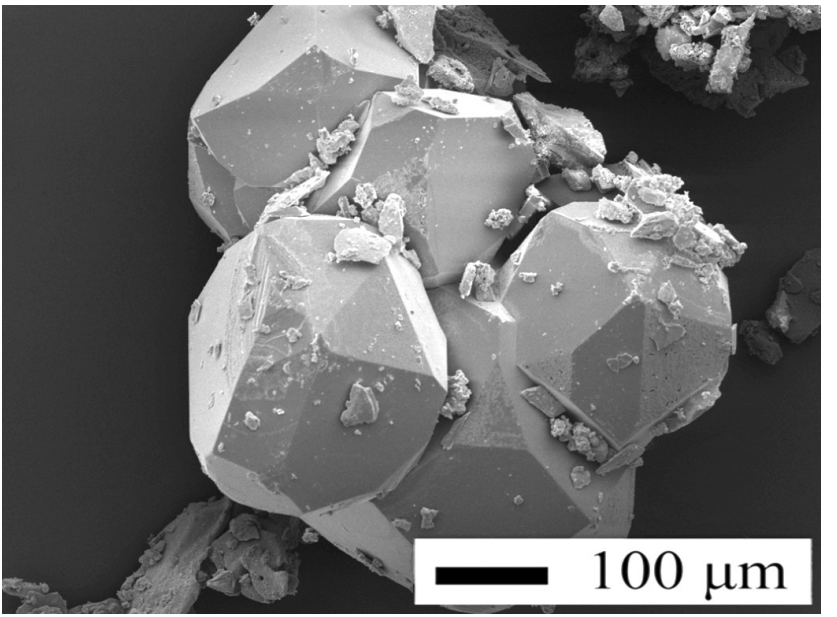

(a)

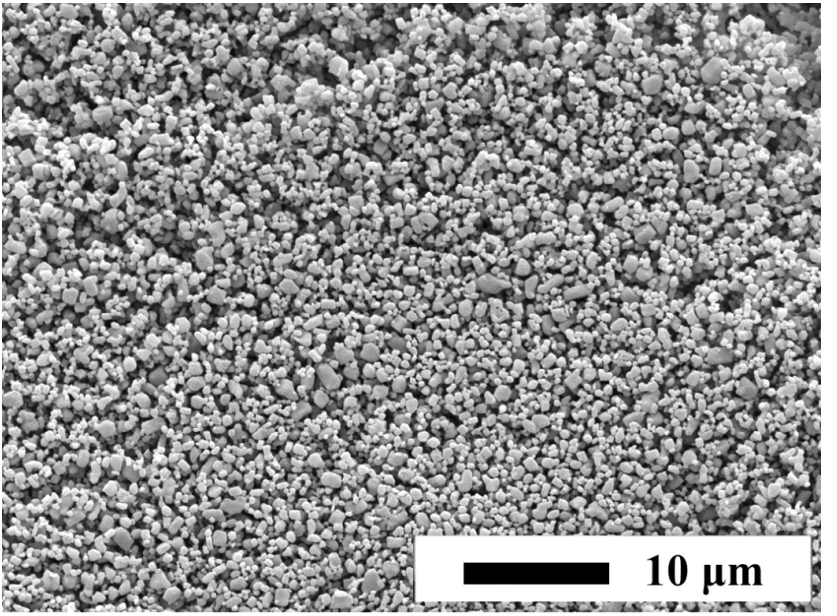

(b)

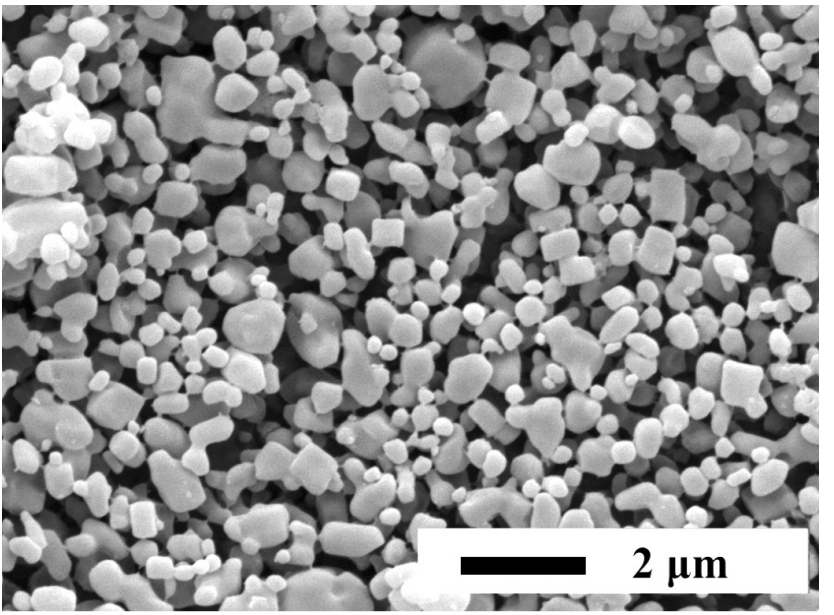

(c)

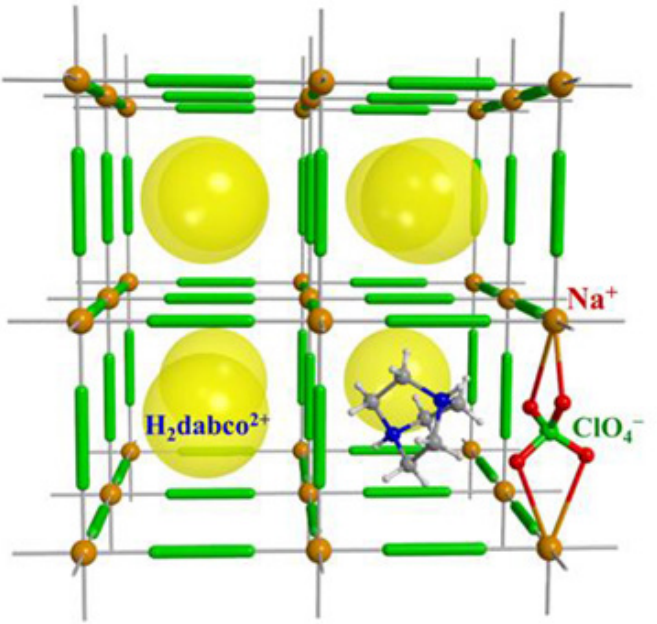

(d)

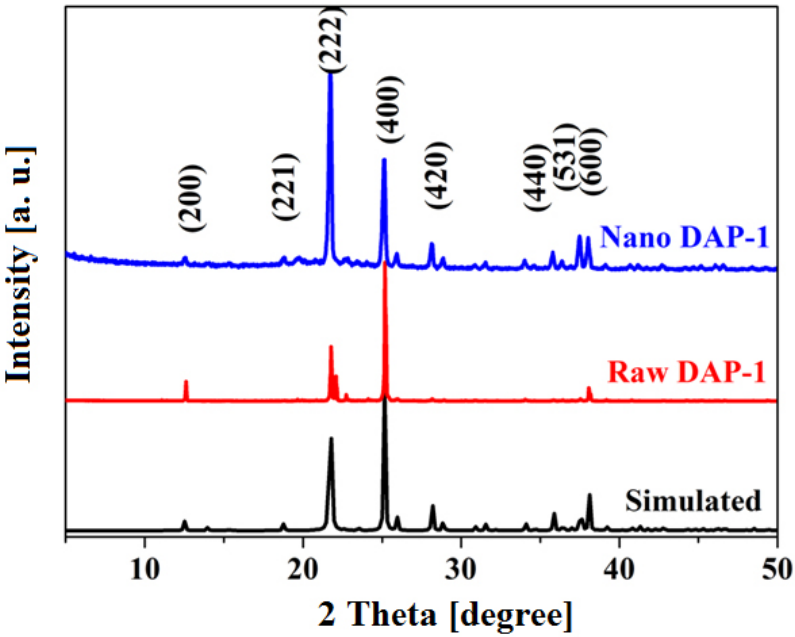

(e)

Figure 1. SEM images of raw (a) and nano DAP-1 (b, c), plus a diagram of the crystal structure (d) and the XRD patterns of DAP-1 samples (e)

In order to further ascertain whether the molecular structure of DAP-1 had changed during the ball-milling process, FT-IR analysis was carried out and the spectra are shown in Figure 2. By the assignment of the peaks discussed, the key functional groups of raw DAP-1, which are located at 1070 cm^{-1}, corresponding to ClO_4^- anions, and peaks at 1050, 891, and 847 cm^{-1}, from the skeletal motion of the protonated H_2dabco^{2+} cations, it was found that the infrared absorption peaks of nano DAP-1 are completely consistent with those of raw DAP-1, although their different transmittances are due to differences in the particle size before and after ball-milling. This revealed that the molecular structure of DAP-1 had not changed, and the molecular structure had high stability during the ball-milling process. Other impurities were not mixed and no other chemical reactions occurred in the preparation process. The thermal decomposition properties of the DAP-1 samples were investigated by differential scanning calorimetry (DSC), and the DSC curves are shown in Figure 3.

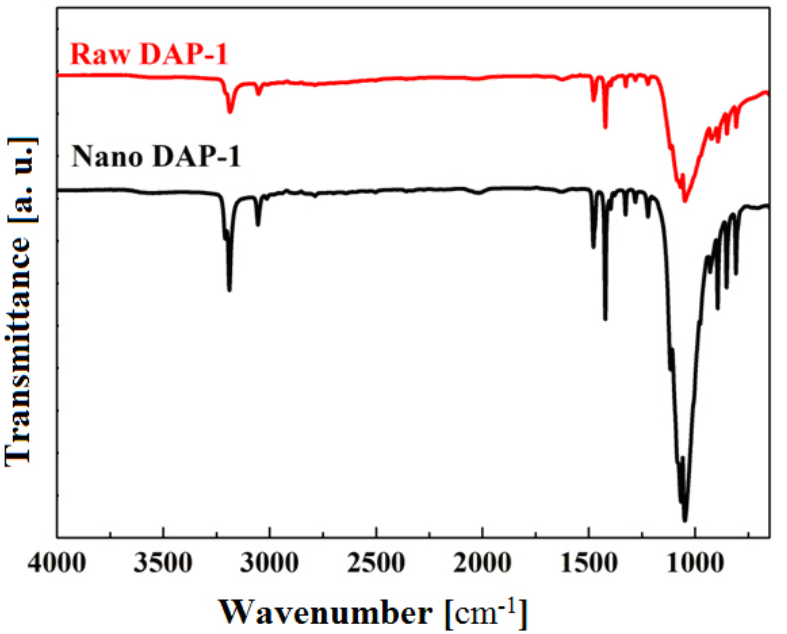

Figure 2. FT-IR spectra of DAP-1 samples: raw (above) and nano DAP-1 (below)

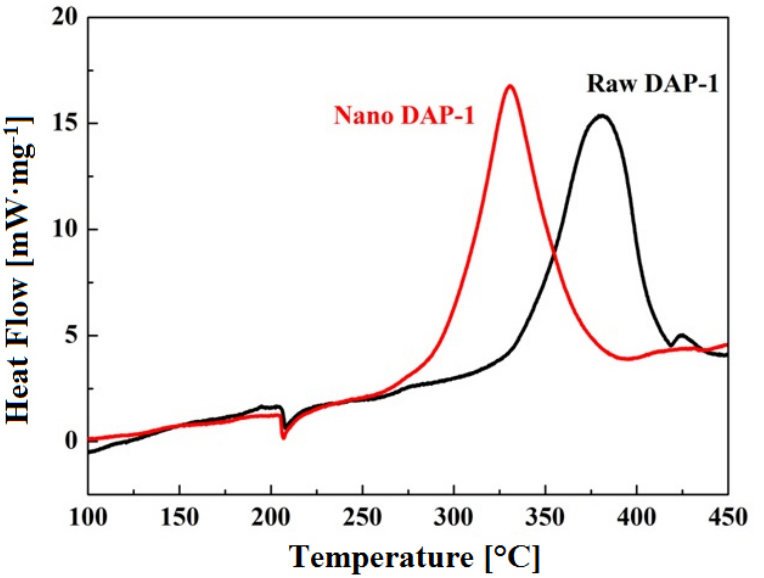

Figure 3. The DSC curves of raw and nano DAP-1 samples

In Figure 3, the first endothermic peak is the phase transformation of DAP-1, and the second exothermic peak is the thermal decomposition of DAP-1. The phase transformation endothermic peak temperature hardly changes. The exothermic peak of nano DAP-1 thermal decomposition was 330.0 °C, a decrease of 51.7 °C compared with raw DAP (381.7 °C).

Figures 4(a)-(c) show the DSC curves of raw DAP-1 and nano DAP-1 at different heating rate (5, 10, 15 and 20 °C·min^{-1}), and the Kissinger plots of $\ln(\beta/T_p^2)$ and $1/T_p$. The apparent activation energy (E_a) of nano DAP-1 was calculated as 160.9 kJ·mol^{-1} by the Kissinger equation (Equation 1) [34, 35], which is lower than that of raw DAP-1 (168.6 kJ·mol^{-1}).

$$\ln\frac{\beta}{T_p^{\,2}} = \ln\frac{R \cdot A_K}{E_K} - \frac{E_K}{R} \cdot \frac{1}{T_p} \tag{1}$$

where T_p is the peak temperature in the DSC curve at heating rate β, β is the heating rate (°C·min^{-1}), E_k reflects the activation energy, A_k represent the pre-exponential factor and R is the gas constant (R = 8.314 J·mol^{-1}·K^{-1}).

The value of E_a can reflect the degree of difficulty of a chemical reaction. A substance with a lower activation energy has a higher reaction rate. Therefore, reducing the activation energy can effectively promote the reaction. The value of E_a for nano DAP-1 was lower than raw DAP-1. The Ozawa method was also used to determine the apparent activation energy [36]. The value of E_a of nano DAP-1 was calculated as 162.7 kJ·mol^{-1} by the Ozawa equation, which is lower than that of raw DAP-1 (170.6 kJ·mol^{-1}) by the same method. For traditional high-energy-density materials, RDX, HMX and CL-20, the E_a values of the thermal decomposition of RDX is 167.24 kJ·mol^{-1} [37], of HMX is 360.6 kJ·mol^{-1} [38], and of CL-20 is 186.55 kJ·mol^{-1} [30]. Thus, the greater the number of activated molecules for nano DAP-1 at a specific temperature, the faster is the decomposition reaction.

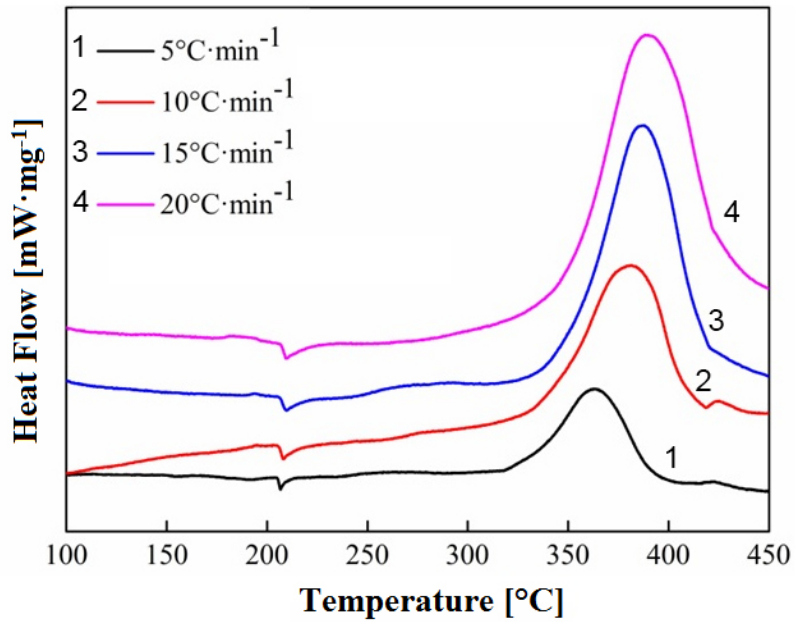

(a)

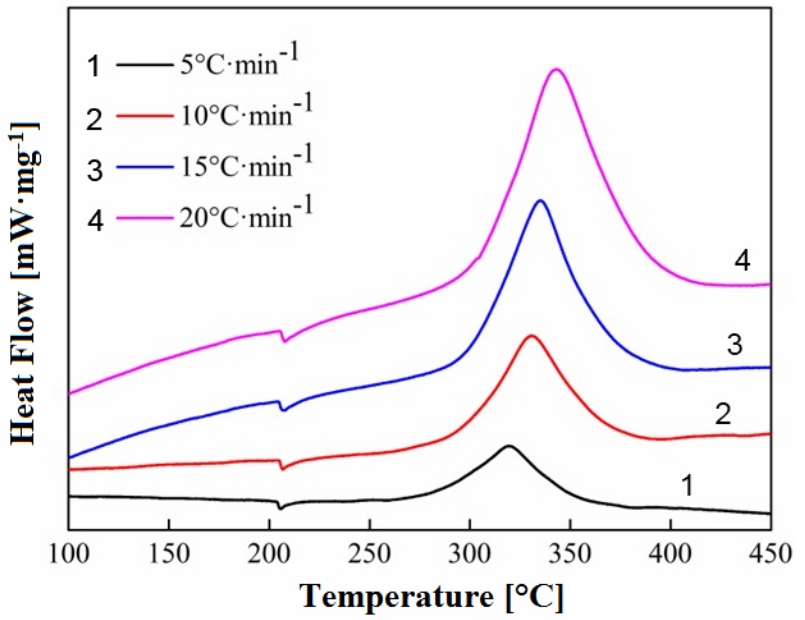

(b)

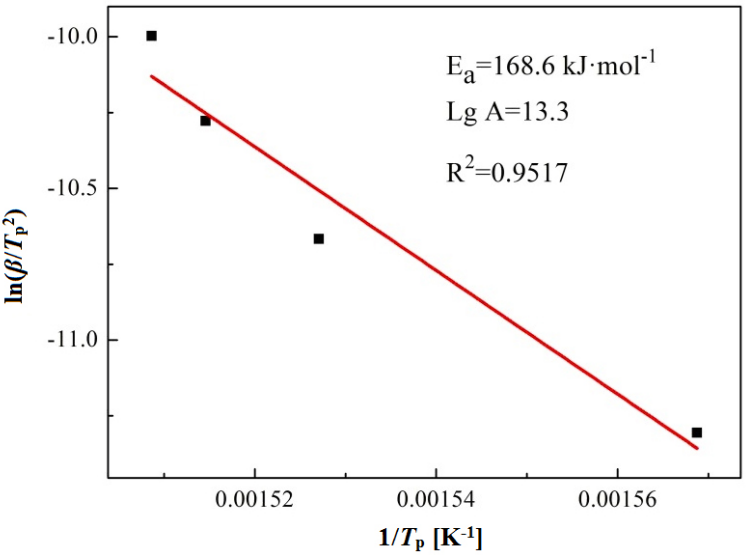

(c)

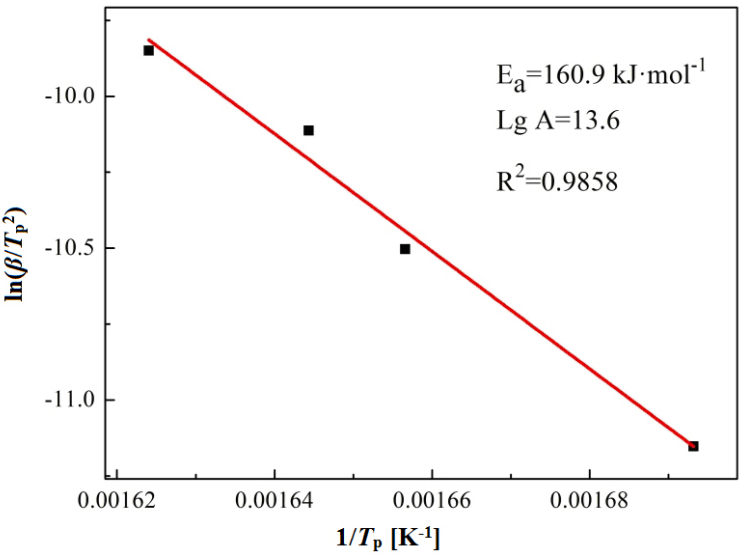

(d)

Figure 4. DSC curves of raw DAP-1 (a), and nano DAP-1 (b) at different heating rates, and the dependence of $\ln(\beta/T_p^2)$ versus $1/T_p$ (c and d respectively) (scatter points are experimental data and the lines denote the linear fitting results)

In order to evaluate the mechanical sensitivity of the samples before and after ball-milling, impact and friction sensitivity tests were performed, and the results are shown in Table 1. Generally speaking, the coordination with metal ions will lead to high sensitivity for mechanical sensitivity. For impact sensitivities, the special height (H_{50}) of the raw sample was 51 cm in this work, indicating that raw DAP-1 with irregular sharp particles exhibited greater sensitivity. After ball-milling, nano DAP-1 had an H_{50} value of 64 cm, less sensitive than the raw material, due to the disappearance of the irregular morphology and the appearance of near spherical nanoscale particles after ball-milling [32]. However, the samples before and after ball-milling had similar sensitivity towards frictional stimuli. The ball-milling technique failed to reduce the friction sensitivity efficiently. This is due to the intrinsic properties of the perovskite structure.

Table 1. Mechanical sensitivity of DAP-1 samples

Sample	Impact sensitivity, H_{50} [cm]	Friction sensitivity, P [%]
Raw DAP-1	51	100
Nano DAP-1	64	100

4 Conclusions

- In summary, mechanical ball-milling technology was introduced to prepare nano DAP-1 with the aim of reducing the mechanical sensitivity.
- The morphology and structure of DAP-1 before and after the ball-milling treatment were studied.
- The thermal decomposition performance of as-obtained samples were discussed and their mechanical sensitivities were evaluated. The exothermic peak of nano DAP-1 was 330.0 °C, a decrease of 51.7 °C compared to raw DAP (381.7 °C). The apparent activation energy (E_a) of nano DAP-1 (160.9 kJ·mol^{-1}), was lower than that of raw DAP-1 (168.6 kJ·mol^{-1}).
- Mechanical sensitivity studies showed that nano DAP-1 (H_{50}: 64 cm) exhibited lower impact sensitivity than raw DAP-1 (H_{50}: 51 cm), although the friction sensitivity was not reduced.
- This work can offer a new way to promote the further application of molecular perovskite energetic materials in advanced explosive and propellant fields.

Acknowledgments

This work was supported by Fundamental Research Program of Shanxi Province (No.: 202101D111175) and Scientific and Technological Innovation Programs of Higher Education Institutions in Shanxi (STIP) (No.: 2019L0517). The authors thank Prof. Weixiong Zhang and Ph.D. Shaoli Chen (School of Chemistry, Sun Yat-Sen University) for support and help.

References

[1] Fei, T.; Lv, P.; Liu, Y.; He, C.; Sun, C.; Pang, S. Design and Synthesis of a Series of CL-20 Cocrystals: Six-membered Symmetrical N-heterocyclic Compounds as Effective Coformers. *Cryst. Growth Des*. **2019**, *19*(5): 2779-2784.

[2] Zhai, L.; Bi, F.; Zhang, J.; Zhang, J.; Li, X.; Wang, B.; Chen, S. 3,4-*Bis*(3-tetrazolylfuroxan-4-yl) Furoxan: A Linear C-C Bonded Pentaheterocyclic Energetic Material with High Heat of Formation and Superior Performance. *ACS Omega* **2020**, *19*(5): 11115-11122.

[3] Lu, F.; Dong, Y.; Fei, T.; Liu, J.; Su, H.; Li, S.; Pang, S. Noncovalent Modification of 4,4′-Azo-1,2,4-triazole Backbone via Cocrystallization with Polynitroazoles. *Cryst. Growth Des*. **2019**, *19*(12): 7206-7216.

[4] Tang, Y.; Huang, W.; Imler, G.H.; Parrish, D.A.; Shreeve, J.N.M. Enforced Planar FOX-7-like Molecules: A Strategy for Thermally Stable and Insensitive π-Conjugated Energetic Materials. *J. Am. Chem. Soc*. **2020**, *142*(15): 7153-7160.

[5] Liu, W.; Lin, Q.; Yang, Y.; Zhang, X.; Li, Y.; Lin, Z.; Pang, S. Energetic Salts Based on an Oxygen-containing Cation: 2,4-Diamino-1,3,5-triazine-6-one. *Chem.-Asian J*. **2014**, *9*(2): 479-486.

[6] Liu, L.; Zhang, Y.; Zhang, S.; Fei, T. Heterocyclic Energetic Salts of 4,4’,5,5’-Tetranitro-2,2’-biimidazole. *J. Energ. Mater.* **2015**, *33*(3): 202-214.

[7] Du, Y.; Su, H.; Fei, T.; Hu, B.; Zhang, J.; Li, S.; Pang, S.; Nie, F. Structure–property Relationship in Energetic Cationic Metal–Organic Frameworks: New Insight for Design of Advanced Energetic Materials. *Cryst. Growth Des*. **2018**, *18*(10): 5896-5903.

[8] Zhao, C.; Du, Y.; Zhang, J.; Mi, Y.; Su, H.; Fei, T.; Li, S.; Pang, S. Highly Efficient Separation of Anionic Organic Pollutants from Water via Construction of Functional Cationic Metal–Organic Frameworks and Mechanistic Study. *ACS Appl. Mater. Inter*. **2020**, *12*(20): 22835-22844.

[9] Yang, Z.; Li, H.; Zhou, X.; Zhang, C.; Huang, H.; Li, J.; Nie, F. Characterization and Properties of a Novel Energetic-energetic Cocrystal Explosive Composed of HNIW and BTF. *Cryst. Growth Des*. **2012**, *12*(11): 5155-5158.

[10] Yang, Z.; Wang, H.; Zhang, J.; Ma, Y.; Tan, Y.; Nie, F.; Zhang, J.; Li, H. Rapid Cocrystallization by Exploiting Differential Solubility: An Efficient and Scalable Process toward Easily Fabricating Energetic Cocrystals. *Cryst. Growth Des*. **2020**, *20*(4): 2129-2134.

[11] Ruesch, M.D.; Powell, M.S.; Satija, A.; Ruesch, J.P.; Vuppuluri, V.S.; Lucht, R.P.; Son, S.F. Burning Rate and Flame Structure of Cocrystals of CL-20 and a Polycrystalline Composite Crystal of HMX/AP. *Combust. Flame* **2020**, *219*: 129-135.

[12] Liu, R.; Chen, P.; Zhang, X.; Zhu, S. Non-Shock Ignition Probability of Octahydro-1,3,5,7-Tetranitro-Tetrazocine-Based Polymer Bonded Explosives Based on Microcrack Stochastic Distribution. *Propellants Explos. Pyrotech*. **2020**, *45*(4): 568-580.

[13] Liu, R.; Wang, X.; Chen, P.; Ge, K.; Zhu, S.; Guo, Y. The Role of Tension-compression Asymmetrical Microcrack Evolution in the Ignition of Polymer-bonded Explosives under Low-velocity Impact. *J. Appl. Phys*. **2021**, *129*(17): 175108.

[14] Chen, S.; Yang, Z.; Wang, B.; Shang, Y.; Sun, L.; He, C.; Zhou, H.; Zhang, W.; Chen, X. Molecular Perovskite High-energetic Materials. *Sci. China Mater.* **2018**, *61*(8): 1123-1128.

[15] Chen, S.; Shang, Y.; He, C.; Sun, L.; Ye, Z.; Zhang, W.; Chen, X. Optimizing the Oxygen Balance by Changing the A-site Cations in Molecular Perovskite High-energetic Materials. *CrystEngComm* **2018**, *20*(46): 7458-7463.

[16] Shang, Y.; Huang, R.; Chen, S.; He, C.; Yu, Z.; Ye, Z.; Zhang, W.; Chen X. Metal-free Molecular Perovskite High-energetic Materials. *Cryst. Growth Des.* **2020**, *20*(3): 1891-1897.

[17] Deng, P.; Ren, H.; Jiao, Q. Enhanced the Combustion Performances of Ammonium Perchlorate-based Energetic Molecular Perovskite using Functionalized Graphene. *Vacuum* **2019**, *169*: 108882.

[18] Jia, Q.; Deng, P.; Li, X.; Hu, L.; Cao, X. Insight into the Thermal Decomposition Properties of Potassium Perchlorate ($KClO_4$)-based Molecular Perovskite. *Vacuum* **2020**, *175*: 109257.

[19] Zhou, J.; Ding, L.; Zhao, F.; Wang, B.; Zhang, J. Thermal Studies of Novel Molecular Perovskite Energetic Material $(C_6H_{14}N_2)[NH_4(ClO_4)_3]$. *Chin. Chem. Lett*. **2020**, *31*(2): 554-558.

[20] Deng, P.; Wang, H.; Yang, X.; Ren, H.; Jiao, Q. Thermal Decomposition and Combustion Performance of High-energy Ammonium Perchlorate-based Molecular Perovskite. *J. Alloy Compd*. **2020**, 827: 154257.

[21] Deng, P.; Ren, H.; Jiao, Q. Enhanced Thermal Decomposition Performance of Sodium Perchlorate by Molecular Assembly Strategy. *Ionics* **2020**, *26*(2): 1039-1044.

[22] Li, X.; Hu, S.; Cao, X.; Hu, L.; Deng, P.; Xie, Z. Ammonium Perchlorate-based Molecular Perovskite Energetic Materials: Preparation, Characterization, and Thermal Catalysis Performance with MoS_2. *J. Energ. Mater.* 2020, *38*(2): 162-169.

[23] Han, K.; Zhang, X.; Deng, P.; Jiao, Q.; Chu, E. Study of the Thermal Catalysis Decomposition of Ammonium Perchlorate-based Molecular Perovskite with Titanium Carbide MXene. *Vacuum* **2020**, *180*: 109572.

[24] Deng, P.; Liu, Y.; Luo, P.; Wang, J.; Liu, Y.; Wang, D.; He, Y. Two-steps Synthesis

of Sandwich-like Graphene Oxide/LLM-105 Nanoenergetic Composites using Functionalized Graphene. *Mater. Lett*. **2017**, *194*: 156-159.

[25] Zhang, H.; Liu, Y.; Li, S.; Huang, S.; Xu, J.; Zhang, H.; Li, J.; Yang, S. Three-dimensional Hierarchical 2,2,4,4,6,6-Hexanitrostilbene Crystalline Clusters Prepared by Controllable Supramolecular Assembly and Deaggregation Process. *CrystEngComm* **2016**, *18*(41): 7940-7944.

[26] Pandita, P.; Arya, V.P.; Kaur, G.; Kumar, R.; Singh, S.; Kumar, M.; Soni, P.K. Size Reduction of HNS to Nanoscale by in Tandem Application of Chemo-mechanical Methods. *Propellants Explos. Pyrotech.* **2019**, *44*(3): 301-312.

[27] Huang, B.; Cao, M.; Nie, F.; Huang, H.; Hu, C. Construction and Properties of Structure-and Size-controlled Micro/Nano-energetic Materials. *Def. Technol*. **2013**, *9*(2): 59-79.

[28] Wuillaume, A.; Beaucamp, A.; David-Quillot, F.; Eradès, C. Formulation and Characterizations of Nanoenergetic Compositions with Improved Safety. *Propellants Explos. Pyrotech*. **2014**, *39*(3): 390-396.

[29] Deng, P.; Jiao, Q.; Ren, H. Nano Dihydroxylammonium 5,5'-Bistetrazole-1,1'-diolate (TKX-50) Sensitized by the Liquid Medium Evaporation-induced Agglomeration Self-assembly. *J. Energ. Mater*. **2020**, *38*(3): 253-260.

[30] Ye, B.; An, C.; Zhang, Y.; Song, C.; Geng, X.; Wang, J. One-step Ball Milling Preparation of Nanoscale CL-20/Graphene Oxide for Significantly Reduced Particle Size and Sensitivity. *Nanoscale Res. Lett*. **2018**, *13*(1): 42.

[31] Qiu, H.; Patel, R.; Damavarapu, R.S.; Stepanov, V. Nanoscale 2CL-20·HMX High Explosive Cocrystal Synthesized by Bead Milling. *CrystEngComm* **2015**, *17*(22): 4080-4083.

[32] Li, F.; Liu, J. Advances in Micro-nano Energetic Materials. *Chin. J. Energ. Mater*. **2018**, *26*(12): 10611073.

[33] Li, T.; Li, R.; Nie, F.; Wang, J.; Huang, W.; Yang, G. Facile Preparation of Self-sensitized FOX-7 with Uniform Pores by Heat Treatment. *Propellants Explos. Pyrotech*. **2014**, *39*(2): 260-266.

[34] Hu, L.; Liu, Y.; Hu, S.; Wang, Y. 1T/2H Multi-phase MoS_2 Heterostructures: Synthesis, Characterization and Thermal Catalysis Decomposition of Dihydroxylammonium 5,5'-Bistetrazole-1,1'-diolate. *New J. Chem*. **2019**, *43*(26): 10434-10441.

[35] Liu, Y.; Hu, L.; Gong, S.; Guang, C.; Li, L.; Hu, S.; Deng, P. Study of Ammonium Perchlorate-based Molecular Perovskite (H_2DABCO)[NH_4(ClO_4)$_3$]/Graphene Energetic Composite with Insensitive Performance. *Cent. Eur. J. Energ. Mater*. **2020**, *17*(3): 451-469.

[36] Jia, Q.; Bai, X.; Zhu, S.; Cao, X.; Deng, P.; Hu, L. Fabrication and Characterization of Nano (H_2dabco)[K(ClO_4)$_3$] Molecular Perovskite by Ball Milling. *J. Energ. Mater.* **2019**: 1-9.

[37] Chen M.H.; Zhang, T.; Chang, W.P.; Jia, X.B. Thermal Decomposition Kinetics of RDX with Distributed Activation Energy Model. *Adv. Mater. Res.* **2013**, 641-642: 144-147.

[38] Elbasuney, S.; Yehia, M.; Hamed, A.; Mohamed Mokhtar, M.; Gobara, M.; Saleh, A.; Elsaka, E.; El-Sayyad, G.S. Synergistic Catalytic Effect of Thermite Nanoparticles on HMX Thermal Decomposition. *J. Inorg. Organomet. Polym. Mater.* **2021**, *31*: 2293-2305.

Received: October 3, 2020
Revised: September 24, 2021
First published online: September 30, 2021